Photon angular distribution of proton-proton bremsstrahlung at 190 MeV

H. Huisman, J. C. S. Bacelar, M. J. van Goethem,* M. N. Harakeh, M. Hoefman, N. Kalantar-Nayestanaki, H. Löhner, M. Mahjour-Shafiei, J. G. Messchendorp,† R. W. Ostendorf, S. Schadmand,† M. Volkerts, and H. W. Wilschut
Kernfysisch Versneller Instituut (KVI), Zernikelaan 25, NL-9747 AA Groningen, The Netherlands

R. S. Simon
Gesellschaft für Schwerionenforschung, Planckstraße 1, D-64291 Darmstadt, Germany
(Received 26 September 2001; published 4 March 2002)

High-precision cross sections and analyzing powers have been measured for proton-proton bremsstrahlung at an incident energy of 190 MeV. A large part of the total reaction phase space has been covered in two separate measurements in which all reaction products were detected. Photon angular distributions for a number of proton angle combinations are presented and compared to theoretical models. The discrepancy between the experimental and theoretical values of the cross sections becomes larger at smaller values of relative energy of the two outgoing protons pointing to the fact that other effects such as those due to the Coulomb force should be investigated more thoroughly. The simplest photonuclear process remains to be fully understood.

The study of nucleon-nucleon (NN) bremsstrahlung, $N+N \rightarrow N+N+\gamma$, has been revived in the past decade with the advent of modern detectors covering a large part of phase space and capable of dealing with high count rates. It is well known that the elastic-scattering cross section of a system can be used to obtain precise scattering amplitudes for *soft*-photon production from the same system [1,2]. The wealth of data on the elastic scattering in the nucleon-nucleon system which has led to very accurate phase shifts in the literature [3,4] can be used for this purpose. If one is interested in dynamical details of the nucleon-nucleon interaction, which are beyond elastic scattering, one has to measure *hard* photons from NN collisions. In nonrelativistic elastic NN scattering, the opening angle between the nucleons is always 90°. Therefore, measurements on NN bremsstrahlung should preferably be performed at small angles, where the opening angle between the two nucleons is also small. At these small angles, one has to deal with large experimental backgrounds and also with very high counting rates from the elastic NN reaction. These problems prevented the small-angle measurements with high accuracy in the past. It can be shown by simple kinematical calculations that, even at intermediate beam energies, one can probe the proton-proton interaction at small relative energies of the outgoing protons. This can be achieved at very small outgoing proton angles which places the kinematics as far away as possible from the elastic channel, but also at larger outgoing proton angles where there is a large asymmetry in the angles. For these kinematics, other effects, such as due to the Coulomb force, which are generally ignored may also become sizable. With the high-precision data from KVI, a detailed investigation of the photon angular distributions can be performed. Exclusive cross sections and analyzing powers for a range of values of relative energies of the two outgoing protons will also be presented for the first time.

For the nucleon-nucleon bremsstrahlung reaction, two types of models will be used to compare the present data with. The first type is the one inspired by the soft-photon theorem [1,2]: the so-called Soft-Photon Amplitudes (SPA) [5,6]. These phenomenological amplitudes use knowledge of the elastic channel to obtain the leading-order terms in the photon energy, but due to the constraint of gauge invariance, other terms beyond the soft-photon theorem are introduced, which partly mimic rescattering and meson exchange contributions. This approximation makes the amplitudes less sensitive to the off-shell structure of the NN interaction. The procedure for including the higher-order terms is not unique and the results can strongly depend on the specific recipe used. The second type of the calculations are microscopic model calculations which are performed in order to investigate the details of the reaction dynamics. These microscopic models can include, in addition to a consistent propagation of the intermediate off-shell nucleons, also higher-order effects like the magnetic meson-exchange currents (MEC) and the virtual Δ isobar [7]. Other calculations, similar to the ones presented here are also available in the literature [8–11].

In this Rapid Communication, we report on the $pp\gamma$ cross sections and analyzing powers as a function of photon polar angle at 190 MeV beam energy. We measured different combinations of proton pairs with very high accuracy in two different experiments. The detection setup measured all three reaction products in coincidence. The total number of good $pp\gamma$ events measured is about 8 million, resulting in the most precise measurement to date on this reaction. Data for only part of the phase space will be presented here. Other selected kinematics addressing other issues have already been published [12,13].

For the measurement of the outgoing protons, the Small-Angle Large-Acceptance Detector (SALAD) was used. This detector was specifically designed and built for these experi-

---

*Present address: National Superconducting Cyclotron Laboratory, Michigan State University, East Lansing, Michigan.

†Present address: Universität Gießen, Heinrich-Buff-Ring 16, D-35392 Gießen, Germany.

ments. The design and operation of this detector are de-scribed in Ref. [14]. It has a large solid angle of 400 msr and allows to make cylindrically-symmetric measurements around the beam axis for most of the polar angular range from 6° to 26°. For the measurement of the bremsstrahlung photons which were detected in coincidence with protons, we used the Two-Arm Photon Spectrometer, TAPS [15]. TAPS consists of approximately 400 BaF$_2$ crystals, which were used in two different geometries in order to cover a large angular range. In the first geometry, all crystals were mounted at backward angles in a large hexagon, surrounding the beam pipe. This results in a polar angular range of 125°−170° and a complete azimuthal coverage. For copla-nar geometries (for the definition of kinematical variables see [16]) presented in this paper, this complete coverage al-lowed us to investigate the results in which the protons have large polar angles, i.e., in the corners of our square-shaped proton detection system. In order to look at a more extensive angular distribution of the photons, a second experiment was performed where the cylindrical symmetry in photon detec-tion was sacrificed. This second geometry consists of six rectangular frames, each containing 64 crystals. These frames were positioned around the target on both sides of the beam pipe. In this geometry the azimuthal range of photon detection at forward angles lies around 0° and 180°.

Because of the high elastic-scattering rate of ≈12 million counts per second for the chosen luminosity, only 2% of the events collected on tape are good bremsstrahlung events, the rest being background that could not be eliminated by the trigger. In order to obtain a clean bremsstrahlung signal from the data, a cut is set on time of flight in TAPS to discriminate massive particles from photons. In addition, the over-determined kinematics of the reaction is used. The three-body final state has nine kinematic variables of which only five are free because of energy and momentum conservation. All nine variables were measured, providing four redundant variables. Since the scattering angles of the three particles are the best measured variables, these angles, except ϕ_γ, are used to reconstruct the three energies and ϕ_γ. As the recon-struction of background events will in general produce for-bidden momenta, reconstruction provides a major reduction of the background. The remaining background is reduced below 1% by using only one of the redundant variables and requiring that the reconstructed and measured values of ϕ_γ do not differ by more than 60°.

The luminosity, the degree of the beam polarization, and efficiencies were obtained in the same way as before [12]. The systematic error on the absolute normalization of the cross-section data is 3%. Point-to-point systematic variations in θ_γ due to geometrical effects in the photon detection sys-tem amounts to a maximum of 5%. This relative error has been added *linearly* to the relatively small statistical errors in the presentation of the data. The error in the analyzing pow-ers is dominated by statistics and small systematic errors have been neglected.

In Fig. 1, the cross sections and analyzing powers are shown as a function of the emitted photon angle for coplanar kinematics and symmetric proton angles ($\theta_1 = \theta_2 \equiv \theta$). In the left panel, where $\theta = 8°$, only data points are shown for θ_γ
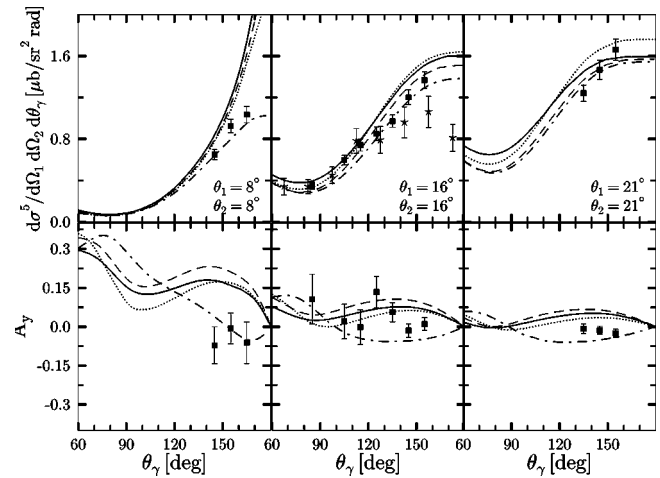
FIG. 1. Cross sections and analyzing powers at symmetric pro-ton angles. Squares represent the results of the present measure-ments. The experimental errors shown in the figure for cross sec-tions (analyzing powers) are, by far, dominated by systematic (statistical) errors. The overall normalization error of 3% is not shown in the figure. However, the angle-to-angle variation of 5% has been added linearly to the statistical errors in the cross sections. The stars are from a TRIUMF measurement at 200 MeV [17]. The dash-dotted line is the result of a SPA calculation, the solid curve is the result of the microscopic model of Martinus *et al.* [7] including all the higher-order corrections, and the dashed curve is the result of the same model without the higher-order corrections. The dotted curve is the result of another microscopic model calculation not including the higher-order effects [20].

>135°. For the bins with a lower θ_γ, one of the protons falls below the detection threshold of SALAD (≈18 MeV), re-sulting in the fact that these bins contain no events. In the middle panel, where $\theta = 16°$, data are available for almost the complete range of θ_γ covered by TAPS. At these kine-matics, cross sections are available from the experiment of Rogers *et al.* [17] performed with an unpolarized proton beam of 200 MeV. These are shown as stars in the top middle panel of Fig. 1. The agreement between our data and this experiment, where there is an overlap, is good. In the right-panel, where $\theta = 21°$, only data from the measurements where the azimuthal-angle coverage is large are available. The bin size in proton angles is in all plots 2°, the bin size in θ_γ is 10° and the bin size in noncoplanarity angle is 5°. The asymmetric cases, where $\theta_1 \neq \theta_2$, for coplanar kinematics are shown in Fig. 2. The combinations of θ_1 and θ_2 are chosen such that data are available for the complete θ_γ range cov-ered. Note that the data sets from the two experiments agreed rather well within statistics and, where kinematically over-lapping, the values were averaged in both figures to produce one experimental point.

The dash-dotted line in both figures is the result of SPA calculations following the recipe outlined by Liou *et al.* [5], which uses the elastic-scattering phase shifts of Ref. [18] as input. The dashed line is the result of a microscopic calcula-tion by Martinus *et al.* [7] in which the off-shell dynamics of the intermediate nucleons has been taken into account in single-scattering and rescattering diagrams. These fully rela-
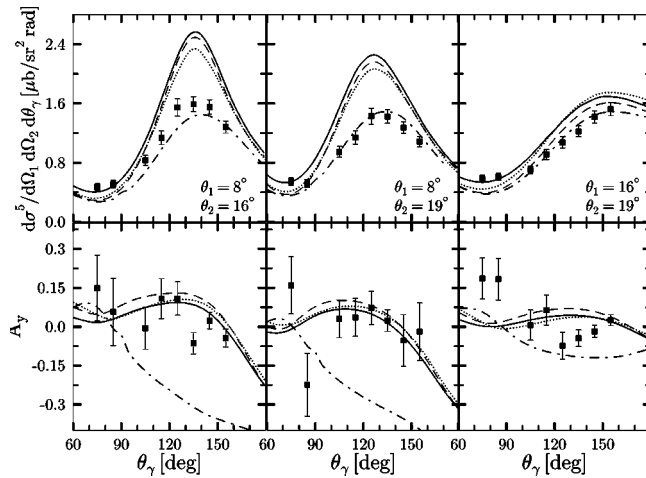
FIG. 2. Same as Fig. 1 except for asymmetric proton angles.

FIG. 3. The absolute value of the difference between the experimental and the theoretical values of the cross sections of Ref. [7] (normalized to the theoretical values) versus the relative energy as defined in the text. The $\triangle$, $\square$, and $\bigcirc$ (open and filled) are for the (symmetric and asymmetric) proton angle combinations of (Figs. 1 and 2) from left to right, respectively. The error bars include the 5% systematic errors as well.

tivistic calculations use the Fleischer-Tjon NN potential [19]. The solid line also includes the higher-order corrections mentioned in the introduction. The dotted line is the calculation based on the work by Herrmann *et al.* [20]. These calculations, which use the Bonn-B potential for proton-proton interaction, include rescattering terms but not the higher-order terms such as the MEC and the Δ-isobar contributions. This curve should then be compared to the dashed line. One would expect two microscopic models with the same ingredients, to predict similar results [21]. The differences in the dashed and dotted curves must then arise primarily from the use of different potentials. None of the calculations include the Coulomb force. The SPA calculation performs best on the cross sections, both at symmetric and asymmetric angles. The microscopic calculations seem to predict the shape of the cross sections reasonably well at large symmetric proton angles. Here, the calculations without the higher-order effects seem to be preferred. However, at small symmetric angle of 8° and large asymmetries in proton angles (the left two panels of Fig. 2), the microscopic models overshoots the cross sections significantly.

A closer inspection of the kinematics of the present experiment reveals that the relative energy of the outgoing two protons varies significantly over the range of the measured variables. The relative energy, $E_{\rm rel}$, is defined by $\sqrt{(E_1+E_2)^2-(\vec{p}_1+\vec{p}_2)^2}-2M_p$, where $E_1(\vec{p}_1)$ and $E_2(\vec{p}_2)$ are the energies (momenta) of protons 1 and 2, respectively, and M_p is the mass of the proton. In particular, if one looks at $E_{\rm rel}$ as a function of the photon angle, one observes that for the symmetric cases, $E_{\rm rel}$ is above 10 MeV everywhere except for the most backward angle of the $\theta_1=\theta_2=8°$ combination. It is also exactly there where the microscopic calculations deviate the most from the cross-section data. For the asymmetric case, one can see that where the microscopic calculations for the cross sections show a strong peak which disagrees with the data, $E_{\rm rel}$ is again below 10 MeV and goes through a minimum. This is all summarized in Fig. 3, where the absolute value of the difference of experimental and theoretical cross sections of Ref. [7] depicted by solid curves in Figs. 1 and 2 (normalized to theoretical cross sections) are shown as a function of $E_{\rm rel}$ for all data points shown in Figs.

1 and 2. Here, one observes a clear increase in the discrepancy between the experimental and the theoretical values as $E_{\rm rel}$ decreases. This was one of the reasons why the Fleischer-Tjon potential, which was known not to provide a good fit to the present-day NN data base and in particular to lower-energy data, had to be revisited. The low-energy behavior of the potential has been changed recently [22]. If one compares the old version of the potential (used in this paper) to the preliminary version of the new fits, one notices that the discrepancy has only been reduced by at most 40% in the region of small $E_{\rm rel}$ and by much smaller amounts elsewhere. Therefore, the trend and the discrepancy still persist. Note that the effect of higher-order terms is minimal where the deviations are largest. Another source of the problem might then be the Coulomb interaction which has been ignored in many calculations so far. A couple of papers addressing this point explicitly conclude that the Coulomb effect should only be considered at *small* proton opening angles where the $^1S_0$ partial wave becomes dominant [20,23,24]. According to these papers, the Coulomb effect cannot be very large in the kinematics presented here except possibly for the $\theta_1=\theta_2=8°$ combination. How small (or large) the Coulomb effect is should be explicitly checked for the kinematics of this paper in lieu of the argument presented above. If the addition of the Coulomb force does not solve the problem, then a serious look has to be taken at the way all the microscopic models are constructed until now. For instance, the approach to satisfy the gauge invariance only approximately [7] must be scrutinized. Another possibility is that the photo-nucleon form factor behaves differently when the nucleon is off its mass shell [25].

The analyzing powers are in general less accurately measured. In the symmetric cases, they are close to zero and more in agreement with the predictions of the SPA calculations. This is in sharp contrast with the asymmetric cases,

where the analyzing powers are clearly better predicted by the two microscopic models and not by the SPA.

In summary, a series of measurements on proton-proton bremsstrahlung have been performed at a beam energy of 190 MeV. The combined statistical and systematic error on the measurements is superior to any prior measurement of this process. For the symmetric proton angles, the present cross-section data are in reasonable agreement with the older data. The microscopic and SPA calculations describe most of the data rather well except at small proton angles. The cross sections for the asymmetric proton angles, on the other hand, generally show sizable differences with the microscopic calculations. For the first time, exclusive cross sections have been accurately measured as a function of the relative energy of the two outgoing protons and down to very small values. Presenting the data as a function of this variable reveals that the discrepancy between the data and the theoretical predictions actually increases with decreasing relative energies. The reason for this is not clear at the moment. It could be still a problem in the low-energy behavior of the potentials used in the calculations, the absence of Coulomb force in the calculations, lack of gauge invariance in the calculations performed or not understanding the photonuclear vertex. Contrary to the cross sections, the analyzing powers are better explained by the microscopic calculations for the asymmetric case. It seems that the simplest photonuclear process is not yet fully understood and needs more theoretical attention.

[1] F.E. Low, Phys. Rev. **110**, 974 (1958).

[2] E.M. Nyman, Phys. Lett. **25B**, 135 (1967); Phys. Rev. **170**, 1628 (1968).

[3] M.C.M. Rentmeester *et al.*, Phys. Rev. Lett. **82**, 4992 (1999).

[4] R.A. Arndt *et al.*, Phys. Rev. C **56**, 3005 (1997).

[5] M.K. Liou, R. Timmermans, and B.F. Gibson, Phys. Rev. C **54**, 1574 (1996); Phys. Lett. B **345**, 372 (1995).

[6] A.Yu. Korchin, O. Scholten, and D. Van Neck, Nucl. Phys. **A602**, 423 (1996).

[7] G.H. Martinus, O. Scholten, and J.A. Tjon, Phys. Lett. B **402**, 7 (1997); Phys. Rev. C **56**, 2945 (1997); Phys. Rev. C **58**, 686 (1998).

[8] J.A. Eden and M.F. Gari, Phys. Rev. C **53**, 1102 (1996).

[9] F. de Jong *et al.*, Phys. Lett. B **333**, 1 (1994); F. de Jong, K. Nakayama, and T.S.H. Lee, Phys. Rev. C **51**, 2334 (1995).

[10] F. de Jong and K. Nakayama, Phys. Rev. C **52**, 2377 (1995).

[11] M. Jetter and H.W. Fearing, Phys. Rev. C **51**, 1666 (1995).

[12] H. Huisman *et al.*, Phys. Rev. Lett. **83**, 4017 (1999).

[13] H. Huisman *et al.*, Phys. Lett. B **476**, 9 (2000).

[14] N. Kalantar-Nayestanaki *et al.*, Nucl. Instrum. Methods Phys. Res. A **444**, 591 (2000), and references therein.

[15] H. Ströher, Phys. News Int. **6**, 7 (1996); A.R. Gabler *et al.*, Nucl. Instrum. Methods Phys. Res. A **346**, 168 (1994).

[16] D. Drechsel and L.C. Maximon, Ann. Phys. (N.Y.) **49**, 403 (1968).

[17] J.G. Rogers *et al.*, Phys. Rev. C **22**, 2512 (1980).

[18] J.R. Bergervoet *et al.*, Phys. Rev. C **41**, 1435 (1990).

[19] J. Fleischer and J.A. Tjon, Nucl. Phys. **A84**, 375 (1974); Phys. Rev. D **15**, 2537 (1977); **21**, 87 (1980).

[20] V. Herrmann *et al.*, Nucl. Phys. **A582**, 568 (1995); K. Nakayama (private communication).

[21] V. Herrmann and K. Nakayama, Phys. Rev. C **45**, 1450 (1992).

[22] D. Cozma, Phys. Rev. C **65**, 024001 (2002); (private communication).

[23] A. Katsogiannis *et al.*, Phys. Rev. C **49**, 2342 (1994).

[24] M. Jetter, H. Freitag and H.V. von Geramb, Phys. Scr. **48**, 229 (1993); Nucl. Phys. **A553**, 665c (1993).

[25] S. Kondratyuk, G.H. Martinus, and O. Scholten, Phys. Lett. B **418**, 20 (1998).